

# Scalable Mobile Fronthaul with Spatial and Spectral Reconfigurability Through Virtually Passive Nodes

Leveraging Flexibility of Access Networks through Software-Defined PON Architectures

Bernhard Schrenk, Thomas Zemen, Martin Stierle, and Helmut Leopold

Dept. Digital Safety & Security / Optical Quantum Technology

AIT Austrian Institute of Technology

Donau-City Straße 1, A-1220 Vienna, Austria

Corresponding author: bernhard.schrenk@ait.ac.at

**Abstract**—A flexible access and mobile fronthaul architecture with spectral re-allocation capability and dynamic lightpath provisioning among network segments is presented. Fully-passive operation of the optical distribution network (ODN) is retained through reconfigurable optical add-drop multiplexers (ROADM) that are solely supplied by means of energy harvesting at the optical layer with a low feed level of -9 dBm. Deployment with a typical power consumption amounting to 90 fJ/bit guarantees an energy-conscious fronthaul technology. It is further proved that urban radio access networks powered by a software-defined optical fronthaul can reduce the required amount of spectral resources by ~26% during on-peak when migrating to 5G.

**Keywords**—Optical fiber communication, Dynamic resource allocation, Passive optical networks, Fronthaul, 5G, Radio access

## I. INTRODUCTION

The advent of 5G and the introduction of next-generation passive optical network (NG-PON2) for wireline optical broadband is bringing a new dawn for optical access networks: for the first time wavelength division multiplexing (WDM) is effectively used in order to boost the capacity of PONs and the mobile backhaul for 5G transport [1, 2]. In this next-generation infrastructure an ~100-fold increase in delivered mobile bandwidth is anticipated. However, the rigid spectral and spatial configuration of network assets at conventional access networks is putting a roadblock for efficient front- and backhaul integration. Dynamic reconfiguration of the physical layer would enable optimum use of available network resources, e.g. for handling hot spots during localized traffic peaks. The potential of operating simple network nodes dedicated to protection and capacity switching by means of energy harvesting has been recently tapped [3].

In this work we exploit the world's first ROADM that operates without field-installed power supply in order to enable a software-defined PON. We show that optical power feeding can be conducted energy-efficiently. Moreover, we proof through a case study in an urban radio access environment that a migration to a flexible yet passive ODN can reduce the amount of required wavelength resources at the fronthaul, thus ensuring scalable network upgrades.

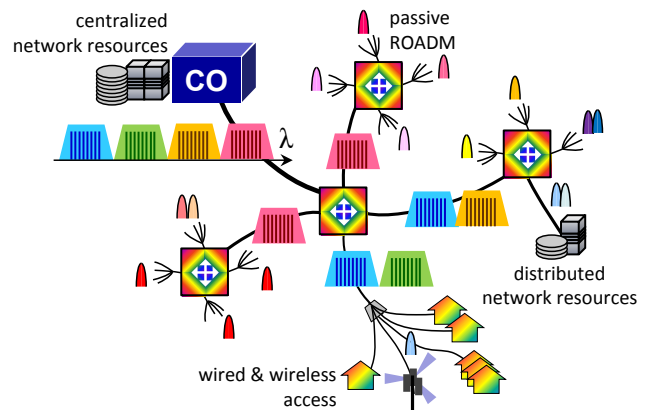


Fig. 1. Introducing resource allocation at the physical layer of wired and wireless access PONs through passive ROADMs as flexible optical splitter.

## II. MIGRATION TO A FLEXIBLE AND SCALABLE FRONTHAUL THROUGH FULLY-PASSIVE ROADM

With migration to 5G the mobile front- and backhaul are of paramount importance for radio access. Foremost its consolidation strength enables cloud-oriented signal processing and recovery. As will be quantitatively pointed out in Section V, a high degree of dynamicity is to be expected at the wavelength level, which demands for reconfigurable add/drop of spectral resources and load balancing mechanisms. Besides, link protection in combination with disaster recovery ensures reliable service delivery while load-dependent off-loading of congested remote radio heads (RRH) to computational resources or micro-servers closer to the users can be supported by the on-demand formation of virtual PONs. On top of this, scalability remains to be a key ingredient for future-proof networks.

The realization of all these functions while avoiding limitations due to optical splitting loss or fixed WDM requires ROADM functionality at a cost-sensitive segment where a passive nature of the network needs to be retained (Fig. 1). Energy scavenging in combination with low-power components can address both requirements, as will be shown shortly. Alongside 5G fronthaul applications the proposed ODN functionality can be beneficial for wired access networks where it can ease network restoration or support multi-

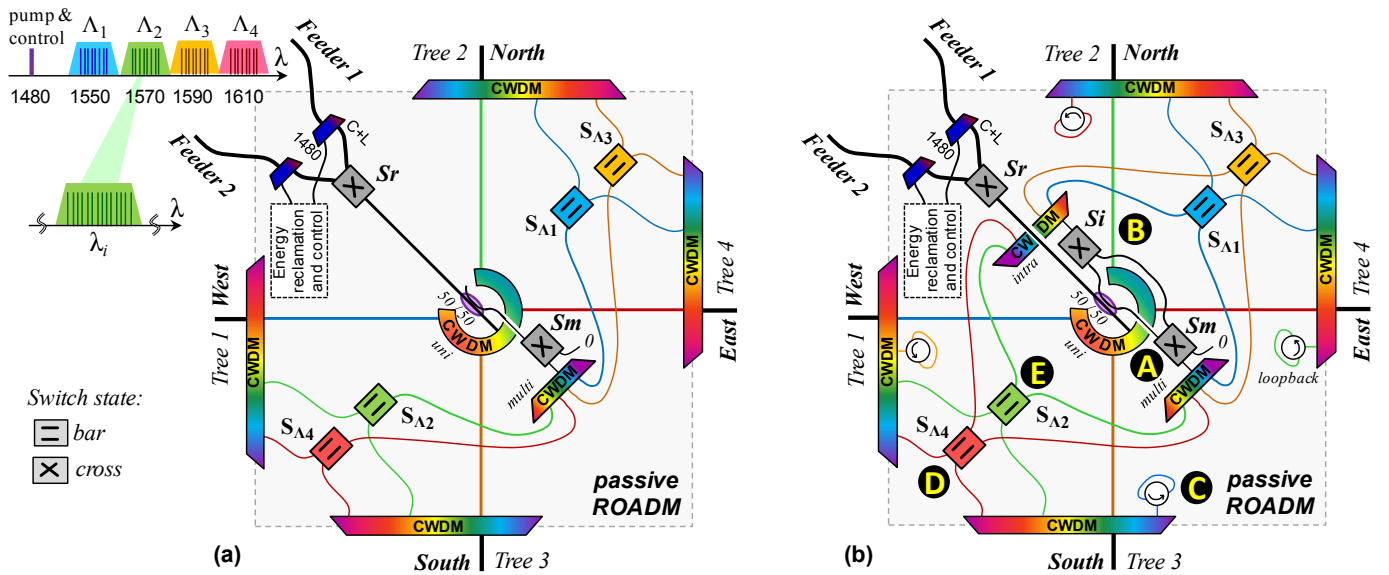


Fig. 2. Architecture of passive ROADM as key element for flexible access, featuring (a) multicast functionality and (b) additional creation of virtual PONs.

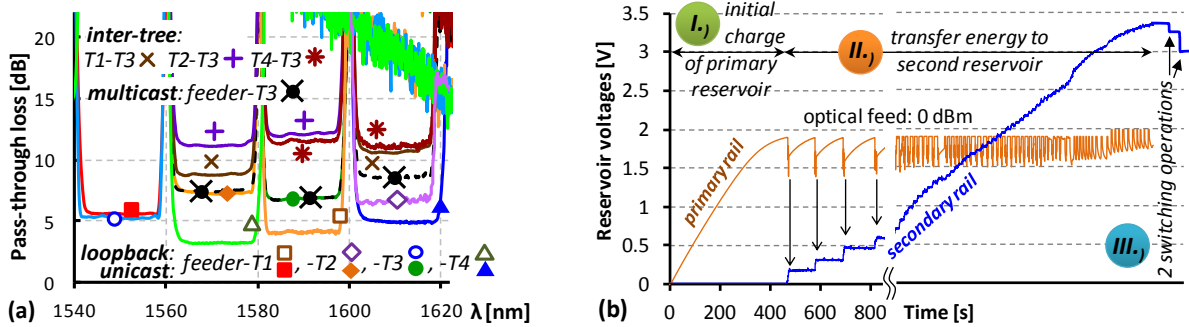


Fig. 3. (a) Transmission functions of individual ROADM lightpaths and (b) optical energy feeding when powering up the ROADM node.

operability by avoiding truck rolls for lightpath reconfiguration in the field.

Figure 2 depicts the proposed architecture of 4-degree nodes able to perform (a) conventional waveband routing with dynamically allocated spectral extension bands and (b) additional virtual PON provisioning among different tree segments. Four wavelength sets  $\Lambda_i$  adjusted to the coarse WDM (CWDM) grid from 1550 to 1610 nm have been used for the demonstration. Within these wavebands, multiple dense WDM (DWDM) channels  $\lambda_i$  can be allocated as intended by the WDM overlay option of NG-PON2. Resiliency is provided in combination with a dual-feeder scheme through the  $2 \times 1$  switch ‘ $S_r$ ’ [3]. Several switches used are based on latching micro opto-electro-mechanic system (MOEMS) technology and do only consume power during actuation [4]. Reconfigurable add/drop is then performed for the four wavelength sets: while each of the wavebands  $\Lambda_i$  is trunked to a certain tree port  $i$  with fixed allocation (Fig. 3(a), unicast), the neighboring wavebands can be spectrally appended to this tree port. For example, the sets  $\Lambda_2$  and  $\Lambda_4$  can be dynamically added to tree port 3 together with  $\Lambda_3$  (Fig. 3(a), multicast). This is achieved by splitting the feeder signal at the node input and a parallel CWDM-reconfigurable ROADM branch incorporating the  $2 \times 2$  MOEMS switches ‘ $S_m$ ’ and ‘ $S_{A_i}$ ’ that enable multicasting and set the output port dedication of the spectral

extension bands  $\Lambda_i$ , respectively. Since wavebands are forwarded to 2 tree ports in this case, a broadcast-and-select scheme at the DWDM level has to be applied at the network units, e.g. by means of tunable filters/lasers. Wavelengths  $\lambda_i$  within the sets  $\Lambda_i$  can be also shared among different trees by means of time division multiplexing.

Conventional head-end to tail-end connectivity can be established at a dedicated waveband (e.g.,  $\Lambda_3$  for tree 3) between central office (CO) and RRHs at cell sites or optical network units (ONU) as wired end-user, remote protocol terminator or distributed network resource. In addition inter-tree PONs can be virtually formed by using unused wavelength sets that are currently not dedicated to a certain tree port, e.g.,  $\Lambda_1$ ,  $\Lambda_2$  and  $\Lambda_4$  in case of tree 3. Wavelengths in these bands are re-routed to other tree ports through a loop along the MOEMS switches ‘ $S_{A_i}$ ’, ‘ $S_i$ ’ and ‘ $S_m$ ’. For example, a connection between trees 1 and 3 can be made at  $\Lambda_2$  (Fig. 3(a), inter-tree  $\times$ ) by setting switch ‘ $S_{A_2}$ ’ in bar-state and routing the signal through switches ‘ $S_i$ ’, ‘ $S_m$ ’ and again ‘ $S_{A_2}$ ’ to the target tree. Finally, intra-tree transmission to/from the same tree segment is established at a circulating loopback path with a dedicated wavelength, e.g.,  $\Lambda_1$  in case of Tree 3 (Fig. 3(a), loopback  $\circ$ ).

The ROADM offering all this functionality uses 7 CWDM multiplexer and 7 MOEMS switches. Although it does not

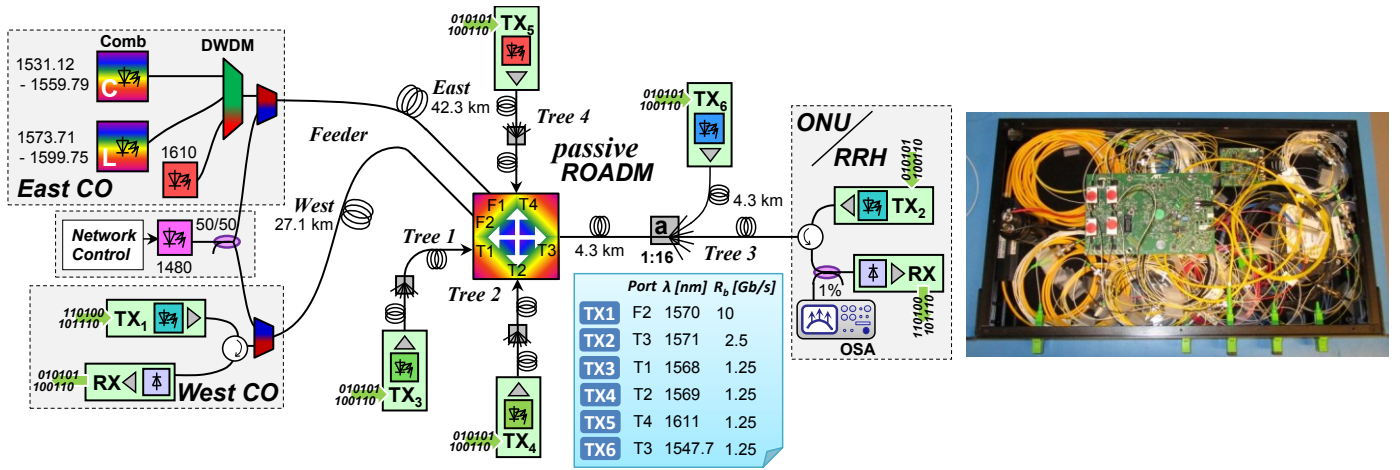


Fig. 4. Experimental setup for evaluating basic functionality of a reconfigurable wireline-wireless access PON. The inset shows the ROADM prototype.

grant all extra features to all tree ports at the same time, it constitutes a good trade-off in view of its passiveness and PON reconfigurability.

A control plane & pump signal at 1480 nm is extracted at the feeder-side interface for remote configuration and powering of the node. An energy harvesting circuit enables fully-passive operation through photovoltaic power conversion by a stack of 4 PIN diodes followed by a capacitive boost converter that charges a 0.13F supercapacitor [3]. Energy cycling and control plane signaling is facilitated through a microcontroller operating at a current of 2  $\mu$ A at 1.6V, which can be guaranteed by an optical feed as low as -9 dBm. A typical charge procedure is shown in Fig. 3(b). The primary supply is first charged for 9 or 55 min in case of optical feeds of 0 and -9 dBm, respectively. Energy is then transferred in  $\sim$ 60 cycles to the secondary supply connected to the MOEMS switches. The applied energy scavenging procedure is reported in [3].

Transmission spectra for ROADM inter-connects between feeder-tree (unicast at fixed  $\Lambda$  and multicast options) and tree-tree (inter- and intra-tree) can be observed from Fig. 3(a). The -3-dB bandwidth of the wavebands is 16.8 nm. The insertion loss for the most critical inter-tree links ranges from 8.7 to 12.1 dB. The highest value occurs when traversing 4 CWDM multiplexers, a 50/50 coupler and 4 MOEMS switches. It is expected that insertion losses can be significantly reduced for fully-spliced ROADMs avoiding angled connectors. When scaling up the port count it can be anticipated that the loss of the ROADM will be much smaller compared to alternative wavelength-flexible solutions such as optical power splitters.

### III. RECONFIGURATION OF SPECTRUM AND LIGHTPATH

The experimental setup to evaluate flexible node functionality is shown in Fig. 4. Spectral resources are re-partitioned between two feeder and four tree segments according to control plane instructions sent from the CO. The feeder segments were 42.3 and 27.1 km long and the tree segments each consisted of passive split and a short reach of 8.6 km. Measurements will be taken at one ONU/RRH location at tree 3, which receives 1.25 Gb/s transmission from ONUs/RRHs at the trees 1, 2 and 4 while a bidirectional down/upstream at 10/2.5 Gb/s can be established with the West

CO. Besides the aforementioned up/downstream and virtual PON signals the fronthaul was further loaded by the East CO with a C- and L-band comb ( $\Lambda_1$ - $\Lambda_3$ ) and an additional channel at 1610 nm in  $\Lambda_4$  in order to demonstrate spectral reconfigurability. The control plane signal for the passive ROADM was transmitted through the 1480-nm pump, which was multiplexed to the CO signals.

Re-allocation of spectral resources and establishment of virtual PONs as requested by the control plane is shown in Fig. 5 as spectrogram at tree 3. Multicast operation is first enabled (point A in Figs. 2(b) and 5) through switch ‘ $S_m$ ’. With this  $\Lambda_2$  is appended to  $\Lambda_3$ , while  $\Lambda_4$  is by default allocated to tree port 1. Virtual PONs between trees 1-3 and 3-4 are then established (B) through switch ‘ $S_i$ ’ at 1568 and 1611 nm, respectively. Intra-tree communication between ONUs/RRHs at tree 3 is supported at 1547.72 nm without further ROADM actuation (C). The virtual PON between trees 3 and 4 is then broken and the available resource  $\Lambda_4$  is used for multicasting from feeder to tree 3. This is achieved by flipping switch ‘ $S_{\Lambda_4}$ ’, which relays the CO signal at 1610 nm to tree 3 (D). Finally, a virtual PON is created for interconnecting trees 2 and 3. Waveband  $\Lambda_2$  is available to serve this purpose and is employed by flipping switch ‘ $S_{\Lambda_2}$ ’. This takes the option for multicasting  $\Lambda_2$  signals of the CO to tree 3; however, a lightpath between trees 2 and 3 is established at 1569 nm (E). In case that 4 operations (A-B, D-E) have to be performed in a short timescale of seconds, as it is the case for the presented scenario, the optical feed needs to be at least -9 dBm in order to guarantee a high initial charge of the energy reservoir that accounts for the drain of reservoir charge for all consecutive switching operations.

Bit error ratio measurements have been carried out for conventional CO-to-ONU/RRH connectivity and for virtual PON configurations between different ONU/RRHs. No reception penalties have been experienced when passing signals through the ROADM.

### IV. ENERGY EFFICIENCY OF AN OPTICALLY FED ROADM

As an alternative to a dedicated pump wavelength, WDM signals passing through the ROADM can be tapped at the feeder port in order to feed the node. The low required power level of -9 dBm permits the use of a small tap ratio of just 10%,

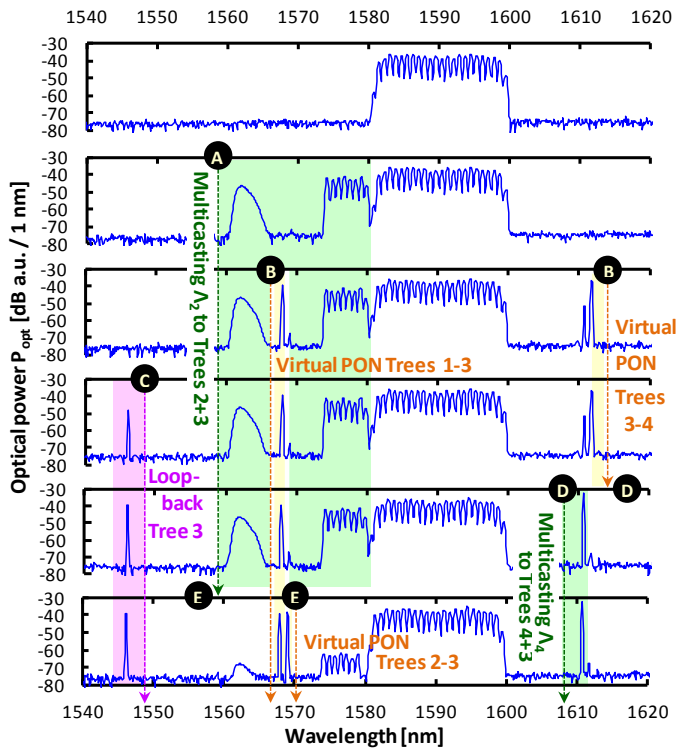


Fig. 5. Spectral reconfiguration and lightpath creation at tree 3.

which corresponds to an insertion loss of  $\sim 0.5$  dB for the WDM signals. This excess loss has to be compensated by a stronger launch per wavelength in order to account for the feeding of the ROADM. In turn the marginally increased drive for the WDM light sources determines the electrical power consumption for the optically fed ROADM as seen by the CO. Figure 6 shows a practical estimation of the required electrical power consumption per ROADM as function of wavelengths per feeder. A nominal launch of 6 dBm/ $\lambda$  and a feeder reach of 20 and 40 km at end-of-life fiber losses of 0.28 dB/km were considered. As can be seen the excess launch for compensating the insertion loss of the feeder tap coupler reduces to below 0.5 dB for an extended fronthaul reach of 40 km and an ensemble of 8 wavelengths (■). This means that the tapped power is strong enough when using a 10% tapping ratio. In case of a short 20 km fronthaul ( $\square$ ) only 2 wavelengths are required to accomplish the optical power feed of the ROADM. This excess loss in the fronthaul is now compensated by increasing the drive settings of the WDM laser bench to provide a 0.5 dB stronger launch. Vertical-cavity surface-emitting laser diodes (VCSEL) were considered since these light sources typically provide the highest slope efficiency. Given representative component characteristics [5] it can be noticed that for the case of 8 fronthaul wavelengths and a 40 km reach an additional electrical power consumption ( $\blacktriangle$ ) of 7.2 mW is experienced for feeding the ROADM optically from the CO. Considering a data rate of 10 Gb/s per wavelength this value translates into an energy consumption of 90 fJ/bit, which as overhead is much smaller than the actual per-bit energy consumption for optical point-to-point transmission. Since the launch has to be increased for every WDM light source ( $\bullet, \circ$ ), an approach with dedicated ROADM pump wavelength can become more favorable for a larger number of fronthaul wavelengths. This

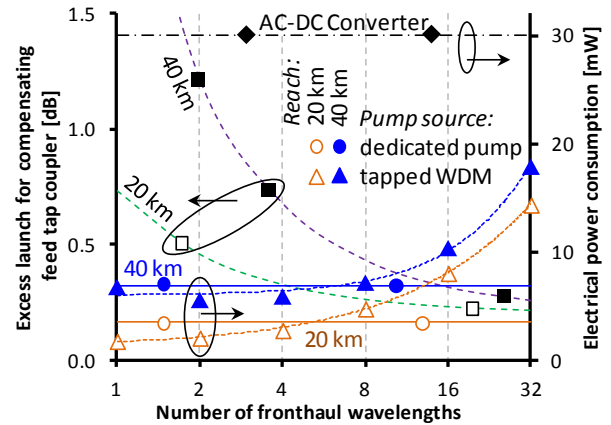


Fig. 6. Power consumption comparison for feeding a ROADM node.

transition is motivated by the low lasing threshold for VCSELs and is reached for 7 wavelengths in case of an extended 40 km reach (intersection  $\blacktriangle, \bullet$ ). It shall be stressed that both optical feeding approaches provide better energy efficiency than a local electrical power supply unit at the ROADM ( $\blacklozenge$ ), which would already exceed previous values with its typical no-load power consumption of 30 mW for AC/DC conversion. Furthermore the obtained consolidation of electrical power supplies at the CO leads to significant cost savings for the roll-out of a flexible ODN.

## V. IMPACT OF USER DYNAMICITY AND DEMAND FOR RESOURCE ALLOCATION AT THE FRONTHAUL

In order to estimate the need for resource re-allocation at the optical layer of radio access networks a case study based on user mobility and migration has been conducted for the urban environment of Vienna, Austria. Five classes of characteristic type of areas have been distinguished for this purpose. The corresponding traffic patterns are presented in Fig. 7(a) and apply to residential districts ( $\bullet$ ), business parks ( $\blacksquare$ ), regions with highly mixed business and residential behavior ( $\blacktriangle$ ), transport areas ( $\blacklozenge$ ) and entertainment locations ( $\blacktriangledown$ ). The patterns are based on average macro-cell load experienced in large scale deployment [6]. After mapping these patterns to the corresponding geographical conditions the cell load has been determined given the actual setup of macro-cells in Vienna. Figure 7(b) shows the resulting load for the urban cell sites over daytime. Different clusters can be observed. Rather constant load is experienced for mixed areas ( $\alpha$ ) for which traffic is continuously generated over daytime. On the contrary business parks ( $\beta$ ) generate load mostly during morning and at noon while towards evening and night there is a sharp drop in required fronthaul capacity. Load is then generated in widespread residential areas ( $\gamma$ ). A variation in traffic can be also observed in cells located near transport areas ( $\delta$ ) for which peaking occurs in the early morning and early evening.

The time-varying traffic of all cell sites has been subsequently aggregated towards a single point of presence. Given the setting for the inner districts of Vienna a large number of 2600 sites are considered to be fronthauled in total. The normalized aggregated load and its variation over daytime are depicted in Fig. 7(c). The load of all macro-cells ( $\square$ )

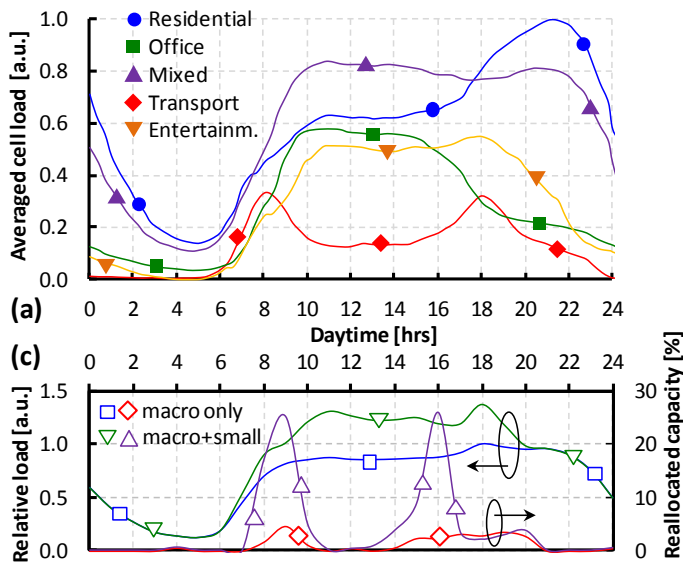


Fig. 7. (a) Traffic patterns, (b) variation of cell loads during daytime, and (c) aggregated fronthaul load and share of re-allocated network capacity.

reaches its maximum in the early evening. As a figure of merit for load dynamics impacting the fronthaul the re-allocation capacity is defined as amount of network resources that are shifted between network segments to maintain network operation without adding capacity through over-provisioning. Re-allocation capacity is therefore experienced under conditions of differential load conditions between segments and a net increase of actual local network load. Despite the strong variation in demand for fronthaul capacity the need for re-allocation for network resources (i.e., wavelengths) between cell sites amounts to only 5% of the total capacity during peak times ( $\diamond$ ). This is explained by the large coverage area of macro cells that require continuous operation even in case of a rather low per-cell bandwidth. Small cells have then been gradually introduced at known hotspots with high congestion. In total 280 small cells have been added, leading to a rather low ratio of 11% between small- and macro-cells. The introduction of cells based on sophisticated beamforming concepts and mm-wave technology changes the scene: Firstly, the required fronthaul capacity ( $\nabla$ ) grows significantly by 40% during on-peak since small-cell technology features  $\sim 10x$  higher baseband modulation bandwidths [1] that result in a higher transmission capacity at the optical fronthaul. Moreover, with their strongly localized nature, small cells are more affected by user mobility and more likely to be activated on-demand. Re-allocation of fronthaul capacity ( $\Delta$ ) by means of switching spectral resources between fronthaul segments therefore becomes more pronounced and reaches a share of up to 26% of actual total capacity. This reflects the need for a flexible ODN at the fronthaul in case that resource overprovisioning has to be avoided. It can be anticipated that re-allocation capacity will surge in more realistic 5G deployments with a larger share of small cells. Furthermore it has to be stressed that other sources of dynamicity have been excluded, such as changes in the topology due to adding and removing network resources for computing and storage, service deployment and support of multi-operability, failure and network restoration, service windows accompanied by traffic rerouting, or weather

conditions that may result in a different mix of access technologies impacting the required fronthaul capacity.

## VI. CONCLUSION

A flexible and scalable wireline-wireless architecture with a passive fiber plant has been demonstrated. It features physical layer reconfigurability for the purpose of dynamic spectrum allocation and formation of virtual PONs. The key enabling element is a fully-passive ROADM powered by energy harvesting at low optical feeds of -9 dBm. This low value permits remote optical feeding with a higher energy efficient than a local power supply unit. The experience overhead in power consumption is in the order of only 90 fJ/bit. Deployment studies on user mobility in realistic urban environments show that a software-defined ODN at the mobile fronthaul can already save up to 26% of spectral resources when just gradually advancing current 4G radio access networks by 5G-flavored small cells.

## REFERENCES

- [1] F. Boccardi, R. Heath, A. Lozano, T. Marzetta, P. Popovski, "Five Disruptive Technology Directions for 5G," *IEEE Comm. Mag.*, vol. 52, p. 74-80, Feb. 2014.
- [2] P. Chanclou, A. Cui, F. Geilhardt, H. Nakamura, D. Nessel, "Network Operator Requirements for the Next Generation of Optical Access Networks," *IEEE Network*, vol. 26, pp. 8-14, Mar. 2012.
- [3] B. Schrenk *et al.*, "Passive ROADM Flexibility in Optical Access with Spectral and Spatial Reconfigurability," *IEEE J. Sel. Areas of Comm.*, vol. 33, pp. 2837-2846, Dec. 2015.
- [4] Y. Bi, J. Jin, A. Dhaini, L. Kazovsky, "QPAR: A Quasi-Passive Reconfigurable Green Node for Dynamic Resource Management in Optical Access Networks," *IEEE/OSA J. Lightwave Technol.*, vol. 32, pp. 1104-1115, Mar. 2014.
- [5] J.F. Seurin *et al.*, "High-power high efficiency 2D VCSEL arrays", in *Proc. SPIE*, vol. 6908, paper 690808, Jan. 2008.
- [6] H. Wang, F. Xu, Y. Li, P. Zhang, D. Jin, "Understanding Mobile Traffic Patterns of Large Scale Cellular Towers in Urban Environment," in *Proc. ACM IMC 2015*, Tokyo, Japan, Oct. 2015, S6.1.